

Conductive Nanoscopic Fibrous Assemblies Containing Helical Tetrathiafulvalene Stacks

Yoko Tatewaki,^{*[a]} Tatsuya Hatanaka,^[b] Ryo Tsunashima,^[d] Takayoshi Nakamura,^[c, d] Mutsumi Kimura,^{*[a, b]} and Hirofusa Shirai^[a]

Abstract: Tetrathiafulvalenes (TTF) *S*-TTF and *R*-TTF having four chiral amide end groups self-organize into helical nanofibers in the presence of 2,3,5,6-tetrafluoro-7,7',8,8'-tetracyano-*p*-quinodimethane (F₄TCNQ). The intermolecular hydrogen bonding among chiral amide end groups and the formation of charge-transfer complexes results in a long one-dimensional supra-

molecular stacking, and the chirality of the end groups affects the molecular orientation of TTF cores within the stacks. Electronic conductivity of a single helical nanoscopic fiber made of

S-TTF and F₄TCNQ is determined to be $(7.0 \pm 3.0) \times 10^{-4} \text{ S cm}^{-1}$ by point-contact current-imaging (PCI) AFM measurement. Nonwoven fabric composed of helical nanofibers shows a semiconducting temperature dependence with an activation energy of 0.18 eV.

Keywords: charge transfer • chirality • helical structures • hydrogen bonds • nanostructures

Introduction

Control of self-assembling processes enhances the properties of molecular materials and devices built-up from functional small molecules.^[1] Many researchers have challenged the design and construction of appropriate supramolecular architectures for desired properties by controlling the intermolecular noncovalent interactions involving hydrogen bonds,

coordination bonds, van der Waals interactions, π - π stacks, and charge-transfer (CT) complex formations. In particular, the assemblies of π -conjugated molecules have attracted special interest because of their great potential for the directional transportation of electrons and energy along with their molecular stacks.^[2] Among the π -conjugated molecules, tetrathiafulvalenes (TTFs) have been widely investigated as molecular metals in crystalline and supramolecular states.^[3] One-dimensional assemblies of CT complexes composed of oxidized TTFs and electron-acceptor molecules show highly electronic conductivities.^[4] Their conductivity strongly depends on the magnitude of the intermolecular CT interactions between the electron-donor and the electron-acceptor molecules, and the length of one-dimensional stacks.^[2,4] Precise control of intermolecular distance within one-dimensional TTF stacks induces the creation of highly conductive molecular materials.

Recently, the formation of supramolecular fibrous organizations has been investigated as gelators.^[5] Low-molecular-weight molecular components assemble into fibrous molecular assemblies, and the gathering of these assemblies forms three-dimensional-network structures. While various functional segments have been introduced into the low-molecular-weight molecular components, there are few reports on the fibrous assemblies consisting of a π -stacked columnar structure of TTFs.^[6] Shinkai and co-workers succeeded in the formation of highly aligned self-assembled TTF fibers.^[7] Kato and co-workers reported the electronic conductivity of

[a] Dr. Y. Tatewaki, Prof. M. Kimura, Prof. H. Shirai
Collaborative Innovation Center for Nanotech FIBER
Shinshu University
Ueda 386-8567 (Japan)
Fax: (+81) 268-21-5499
E-mail: ytatewa@shinshu-u.ac.jp
mkimura@shinshu-u.ac.jp

[b] T. Hatanaka, Prof. M. Kimura
Department of Functional Polymer Science
Faculty of Textile Science and Technology
Shinshu University, Ueda 386-8567 (Japan)

[c] Prof. T. Nakamura
Graduate School of Environmental Earth Science
Hokkaido University
Sapporo 060-0810 (Japan)

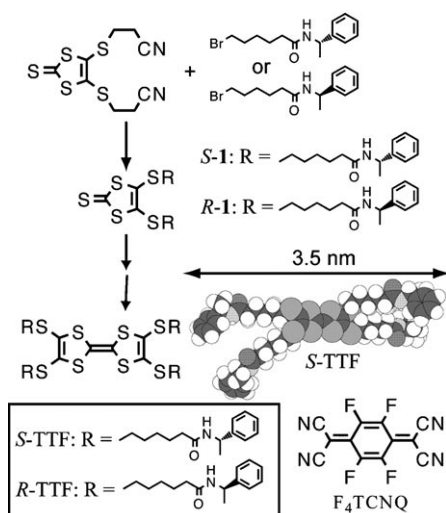
[d] Dr. R. Tsunashima, Prof. T. Nakamura
Research Institute for Electronic Science
Hokkaido University
Sapporo 060-0812 (Japan)

Supporting information for this article is available on the WWW under <http://dx.doi.org/10.1002/asia.200900044>.

self-assembled fibers consisting of TTF-based low-molecular-weight gelators.^[8] Very recently, Iyoda and co-workers reported highly conductive self-assembled fibers from a disk-like TTF hexamer.^[9] These self-assembled fibers based on the stacks of TTF molecules can apply to the construction of conductive nanowires.^[10] However, no conductivities of single self-assembled fibers were measured. We report here the formation of long fibers of molecular diameter and micrometer length containing TTF stacks. The combination of intermolecular hydrogen bonding and charge-transfer complex formation may lead to the formation of stable TTF stacks. The electronic conductivities of self-assembled fibers containing stable TTF stacks were measured by PCI-AFM.

Results and Discussion

Tetrathiafulvalenes bearing four (*R*)- and (*S*)-methylbenzylamide end groups, *R*-TTF and *S*-TTF, were prepared by following the reaction sequence given in Scheme 1.^[11] The



Scheme 1.

key starting material, 4,5-bis(2'-cyanoethylthio)-1,3-dithiole-2-thione, was reacted with hexylbromide, possessing an (*S*)-methylbenzylamide end group, in the presence of CsCO₃ to yield compound *S*-1, which was subsequently converted into the 1,3-dithiol-2-one derivative *S*-2 by reaction with Hg(OAc)₂. The conversion of *S*-2 into the target *S*-TTF was achieved by the reaction in triethyl phosphite at 110 °C, which produced *S*-TTF as an air-stable orange powder. *R*-TTF was synthesized by the same procedure as that for *S*-TTF. All the compounds were fully characterized by MALDI-TOF-mass spectra, and ¹H and ¹³C NMR spectra.

When *S*-TTF was dissolved in hot toluene and then cooled to room temperature, a loose gel was formed, indicating the formation of aggregated *S*-TTF in solution. A TEM image of the loose gel showed spherical objects having 100–200 nm diameters (see Figure S1 in the Supporting In-

formation). In contrast, the stoichiometric mixture of *S*-TTF and the electron-acceptor F₄TCNQ yielded a stiff dark-colored gel. The solution color of *S*-TTF did not change by mixing with 2,5-difluoro-7,7',8,8'-tetracyanoquinodimethane (F₂TCNQ) and 7,7',8,8'-tetracyanoquinodimethane (TCNQ), suggesting that charge transfer from *S*-TTF to these TCNQ derivatives did not occur (see Figure S2 in the Supporting Information). The color change indicates the oxidation of TTF molecules by the addition of F₄TCNQ and the formation of a CT complex between *S*-TTF and F₄TCNQ. The morphology of aggregates changed from spheres to twisted fibers as observed by TEM and AFM (Figure 1a and 1d).

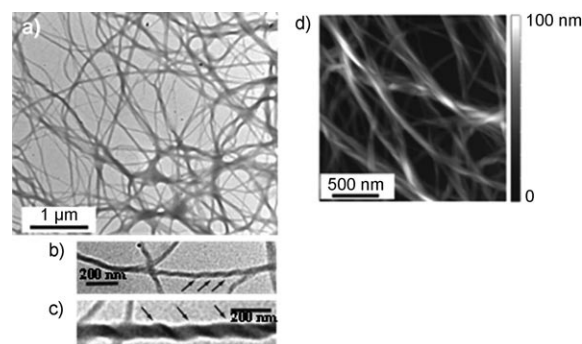


Figure 1. a) and b) Transmission electron micrographs of assemblies made of the stoichiometric mixtures of *S*-TTF with F₄TCNQ, c) *R*-TTF with F₄TCNQ (bar=200 nm). d) AFM image of helical nanofibrous assemblies made of *S*-TTF and F₄TCNQ.

The diameter of the fibrous assemblies was approximately 30–60 nm and the length of fibers was above 10 μm. The mixture of *S*-TTF and F₄TCNQ aggregated to form left-handed helical assemblies with a 60 nm helical pitch as analyzed by TEM (Figure 1b). In contrast, *R*-TTF and F₄TCNQ formed opposite right-handed helical fibers as shown in Figure 1c. The details of the molecular information in the helical fibers has been analyzed by UV/Vis/NIR spectroscopy, FTIR spectroscopy, cyclic voltammetry (CV), ESR, CD spectra, and powdered XRD patterns.

The electronic spectra in the UV/Vis/NIR and IR region for the gel of *S*-TTF and F₄TCNQ were measured (Figure 2). The gel exhibited a broad absorption band in the IR region (2500–3500 cm⁻¹), which is attributable to the

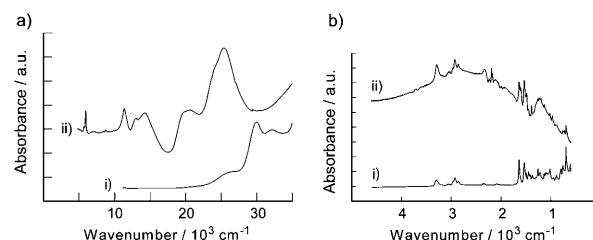


Figure 2. a) UV/Vis/NIR of i) *S*-TTF and ii) mixture of *S*-TTF with F₄TCNQ. b) FTIR spectrum for toluene gel of i) *S*-TTF and ii) mixture of *S*-TTF with F₄TCNQ.

charge transfer between electron-donating TTFs and electron-accepting F_4TCNQ .^[12] The absorption band in the NIR region was unambiguously assigned to the F_4TCNQ anion radicals. A cyclic voltammetric study was performed on *S*-TTF in a dry, degassed acetonitrile solution (see Figure S3 in the Supporting Information). The homogeneous solution of *S*-TTF displayed two reversible one-electron-oxidation waves at $E_{1/2} = +0.45$ and $+0.89$ V versus SCE in the anodic window, which indicated the formation of stable radical cations. These redox potentials almost coincided with those of alkyl-substituted TTFs, which lack chiral amide groups.^[13] Because the redox potential for the oxidation of F_4TCNQ ($+0.70$ V vs SCE) was higher than the first oxidation potential of *S*-TTF, the TTF segment could be oxidized to the radical cation by the addition of F_4TCNQ . The ν_{CN} band was observed at 2193 cm^{-1} in the FTIR spectrum of the dried gel. Because the ν_{CN} bands for neutral F_4TCNQ and F_4TCNQ^- anion radicals have been observed at 2227 and 2193 cm^{-1} , respectively, the observed electronic ground state of the complex was close to a completely ionic state.^[14] The supramolecular gel of *S*-TTF and F_4TCNQ in toluene exhibited an ESR signal at room temperature, also indicating the generation of radical species (see Figure S4 in the Supporting Information). The line width was around 0.44 mT, and the g value was 2.0047 . The g values for bis(ethylenedithio)-tetrathiafulvalene (BEDT-TTF) cation and the F_4TCNQ anion radicals have been reported to be at 2.007 and 2.0025 , respectively.^[15] The observed g value was the intermediate between BEDT-TTF cation and F_4TCNQ anion radicals, revealing that the supramolecular gel consists of the charge-transfer complex between the *S*-TTF cation and F_4TCNQ anion radicals. These results supported the formation of charge-transfer complexes by the electron transfer from TTF to F_4TCNQ within the fibrous assemblies.

The FTIR spectrum of the gel composed of *S*-TTF and F_4TCNQ showed that the 1535 and 1639 cm^{-1} peaks are assignable to the amide groups, indicating that the hydrogen-bonding network is formed among the chiral side chain.^[16] Thus, *S*-TTF can be assembled through two different noncovalent interactions: charge-transfer complex formation and hydrogen bonding. The formation of the hydrogen network among the chiral side chains may affect the molecular arrangement of TTF stacks. Although the CD spectrum of the loose gel of only *S*-TTF was almost silent, the gel of *S*-TTF and F_4TCNQ exhibited CD activities corresponding to every absorption band (Figure 3). The Cotton effect centered at

389 nm can be ascribed to helical dipole coupling between oxidized TTF rings through the hydrogen-network formation of peripheral chiral amides.^[17] In contrast, the gel of *R*-TTF and F_4TCNQ showed a mirror CD spectrum to that of *S*-TTF and F_4TCNQ , indicating the opposite molecular arrangement of TTF rings within the stacks. XRD patterns of the nanofiber composed of the TTF derivative- F_4TCNQ were characterized by three reflection peaks, 3.27 , 1.56 , and 0.99 nm , which were in the ratio of $1:1/2:1/3$ (see Figure S5 in the Supporting Information). These diffraction patterns indicate that the nanofiber of TTF- F_4TCNQ consists of a lamellar structure. The observed spacing at 3.27 nm indicates the width of one layer of the lamellar structure. Judging from the molecular dimension of *S*-TTF, as estimated from the computer-generated molecular model (Scheme 1), the interlamellar distance observed in the XRD study is close to the estimated length of *S*-TTF (3.3 nm). From these results, we can conclude that the hierarchical molecular organization of synthesized TTF molecules is a combination of the formation of one-dimensional charge-transfer stacks and hydrogen bonding among chiral amide groups. Moreover, the chirality affects the molecular orientation of TTFs within the stacks.

Since the discovery of metallic properties in a tetracyano-*p*-quinodimethane (TCNQ) complex of TTF over a relatively wide temperature range, extensive work has been carried out in the design of organic metals and superconductors of CT complexes.^[18] Precise control of the molecular arrangement in CT complexes is essential for obtaining highly conductive organic materials.^[19] The electrical conductivity of the supramolecular gel of *S*-TTF- F_4TCNQ was measured by using evaporated gold electrodes with a gap distance of $500\text{ }\mu\text{m}$. The substrate was fully covered with the organic film by drop-casting the diluted gel solution. The film thickness and the covering ratio of the organic film on the electrode were measured by SEM and AFM measurements. The electrical conductivity of the organic film was $5.0 \times 10^{-4}\text{ Scm}^{-1}$ at room temperature. Akutagawa et al. reported the electronic conductivities of molecular nanowires composed of the CT complex of a TTF-substituted macrocycle and F_4TCNQ .^[20] The obtained value for the electrical conductivity was almost the same as the reported value, suggesting that the three-dimensional network structures of nanofibers provide pathways for electron transportation. The films showed a semiconducting behavior in the measurement of the temperature dependence of the electrical conductivity (σ_{RT}) value, and the activated energy (E_a) obtained from the slope was found to be 0.18 eV (Figure 4a).

The electrical conductivity of each individual nanofiber was measured by PCI-AFM. The PCI-AFM method developed by Kawai and co-workers is a useful technique for measuring I - V characteristics in nanoscale materials.^[21] This method can simultaneously measure the nanostructure and electrical properties of a material on the insulated substrate. The electrical properties of single-wall carbon nanotubes (SWNTs), DNA, and porphyrin assemblies adsorbed on SWNTs have been successfully evaluated by the PCI-AFM

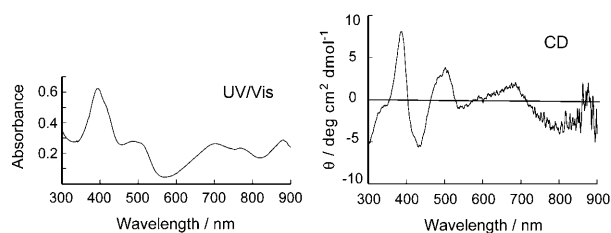


Figure 3. UV/Vis and circular dichroism spectra of toluene gel of *S*-TTF and F_4TCNQ at room temperature.

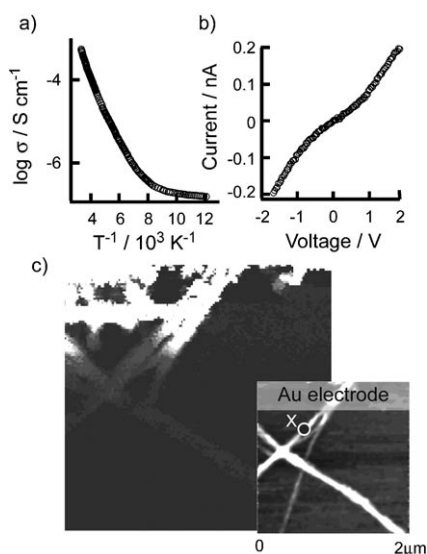


Figure 4. a) Temperature-dependence of electrical conductivity (σ_{RT}) value for the film made of *S*-TTF and F_4TCNQ on the gold electrodes having an electrode gap of 500 μm . b) I - V characteristics by PCI-AFM at the point X in the topographic image as shown in the inset of Figure 4c. c) Current image obtained by PCI-AFM of a nanofiber made of *S*-TTF and F_4TCNQ . The inset shows the topographic image of the same region as the current image.

method.^[22] We also applied this method to measure the electrical conductivities of individual nanofibers composed of CT complexes between an *S*-TTF derivative and F_4TCNQ . Topographic and current images of the cast film are shown in Figure 4c, and the I - V curve at point X on the nanofiber is shown in Figure 4b. The sample was covered with a gold electrode on the left side to form an electrical contact with the nanofibers. The length of the nanofibers was above 1.0 μm and their height was about 15–30 nm, as determined by the topological image. The current image indicates the spatially resolved current map at a bias voltage of 1.8 V. The current image is uniform as is the topological image, and the current image gradually becomes darker with increasing distance from the gold electrode. One-dimensional resistivity can be estimated from the slope of the I - V curve, the distance between the gold electrode and the point contacting the conductive AFM tip, and the cross-sectional area of the nanofiber. The resistivity at the point on the single nanofiber was estimated to be $(7.0 \pm 3.0) \times 10^{-4} \text{ S cm}^{-1}$.

Conclusions

In conclusion, we have demonstrated that the amphiphilic TTFs having chiral side chains can form conductive helical nanofibers in solvents through spontaneous self-assembly processes. The hydrogen bonding of chiral side chains and the CT complex formation have been shown to be the main driving forces for the formation of long and flexible nanofibers, which contain one-dimensional stacks made of oxidized

TTFs and F_4TCNQ . The mechanistic pathway of the self-assembly processes are postulated in Figure 5. The synthesized TTFs assemble into one-dimensional stacks by the formation of CT complexes with F_4TCNQ and intermolecular hy-

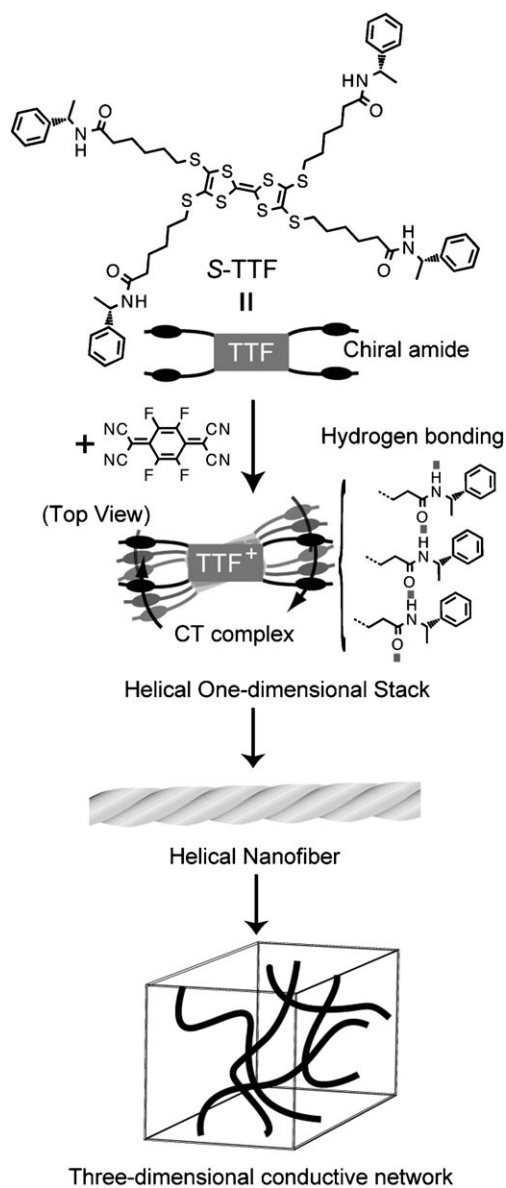


Figure 5. Schematic illustration of the formation of conductive nanoscopic fibers of TTF having chiral side chains in the presence of F_4TCNQ .

drogen bonding among the chiral amide end groups. The intermolecular hydrogen bonding surrounding the one-dimensional stack affects the orientation of the TTFs. The organization of one-dimensional stacks forms long helical nanofibers with approximately 30–60 nm diameters and above 10 μm length. Finally, the partial cross-linking of these helical nanofibers results in a physical gelation. Large network structures of conductive nanofibers will open new possibilities for the construction of soft electronic nanocircuits such as neuronal networks.

Experimental Section

General

NMR spectra were recorded on a Bruker AVANCE 400 FT NMR spectrometer at 399.65 MHz and 100.62 MHz for ^1H and ^{13}C in CDCl_3 solution. Chemical shifts are reported relative to internal TMS. Supramolecular assemblies were transferred onto quartz substrates for UV/Vis/NIR, FTIR, and CD measurements. FTIR spectra were obtained on a Shimadzu IR Prestige-21 spectrophotometer with DuraSample IR II. UV/Vis spectra were measured on a Jasco V-650 and UV/Vis/NIR spectrum was measured on a Hitachi U-4100 spectrophotometer. CD spectra were measured on a Jasco J-720 spectrophotometer at room temperature. MALDI-TOF mass spectra were obtained on a PerSeptive Biosystems Voyager-De-Pro spectrometer with dithranol as matrix. TEM were observed in a JEOL JEM-2010 electron microscope at an acceleration voltage of 200 KV without any staining. The specimens for TEM were prepared by drop-casting of toluene solutions of **1** onto amorphous carbon-coated copper grids (400 mesh). AFM images were obtained using a JEOL 5400 scanning probe microscope operating under the dynamic force mode. Redox potentials were obtained by using CV, and the experimental was carried out in dry degassed acetonitrile solutions of $n\text{Bu}_4\text{NBF}_4$ (0.1 M). The XRD patterns were recorded on a Rigaku Geigerflex diffractometer with $\text{CuK}\alpha$ radiation.

Materials

All chemicals were purchased from commercial suppliers and used without further purification. Column chromatography was performed with activated alumina (Wako, 200 mesh) or Wakogel C-200. Recycling preparative gel permeation chromatography was carried out by a JAI recycling preparative HPLC using CHCl_3 as an eluent. Analytical thin-layer chromatography was performed with commercial Merck plates coated with silica gel 60 F₂₅₄ or aluminum oxide 60 F₂₅₄.

S-1: A solution of $\text{CsOH}\cdot\text{H}_2\text{O}$ (80 mg, 0.48 mmol) in methanol (0.6 mL) was added to a solution of 4,5-bis(2'-cyanoethylthio)-1,3-dithiole-2-thione (66 mg, 0.22 mmol) in acetonitrile (5.5 mL) over 10 min with stirring at room temperature. After stirring for 30 min, hexylbromide having (S)-methylbenzylamide end group^[17a] (500 mg, 1.73 mmol) was added, and the reaction mixture was stirred for 24 h. The reaction mixture was concentrated in vacuo, and water (50 mL) was added. The aqueous solution was extracted with CH_2Cl_2 and the combined organic layer was washed with water. After drying with NaSO_4 , the solvent was evaporated, and the residue was purified by column chromatography (silica, $\text{CH}_2\text{Cl}_2/\text{MeOH}$ 98:2), to afford **S-2** as an orange powder (0.15 g, 63%). FTIR (ATR): $\tilde{\nu}=3304$ (-NH-), 2972 ($-\text{CH}_2-$), 1643 cm^{-1} ($-\text{C}=\text{O}$); ^1H NMR (400.13 MHz, CDCl_3): $\delta=7.29$ (m, 10H, Ar-H), 5.11 (q, $J=7.2$ Hz, 2H, $\text{NH}(\text{CH}_3)\text{CH}(\text{Ar})$), 2.85 (t, $J=7.2$ Hz, 4H, $-\text{SCH}_2\text{CH}_2-$), 2.16 (t, $J=7.6$ Hz, 4H, $-\text{CH}_2\text{CH}_2\text{CO}-$), 1.68 (m, 6H, $-\text{CH}(\text{CH}_3)$), 1.47 ppm (m, 12H, $-\text{CH}_2-$); ^{13}C NMR (100.61 MHz, CDCl_3): $\delta=21.81$, 25.11, 28.09, 29.42, 36.49, 36.66, 48.77, 126.23, 127.39, 128.71, 143.44, 171.59, 207.9 ppm; MS (MALDI-TOF): m/z (%) calcd for $\text{C}_{31}\text{H}_{40}\text{N}_2\text{O}_2\text{S}_5$: 632.99 $[M+H]^+$; found: 634.20.

S-2: A mixture of **S-1** (0.24 g, 0.38 mmol) and $\text{Hg}(\text{OAc})_2$ (0.62 g, 1.98 mmol) in the mixed solvent of CHCl_3 (4.9 mL) and AcOH (2.5 mL) was stirred under N_2 at room temperature for 16 h. The resulting white precipitate was filtered by celite and washed thoroughly with CHCl_3 . The combined organic phases were refluxed with activated charcoal, cooled to room temperature, and filtered. The filtrate was washed with NaHCO_3 solution (4 \times 200 mL), H_2O (200 mL), and was dried over MgSO_4 . The organic layer was evaporated to dryness to afford **S-2** as an orange powder (230 mg, 99%). FTIR (ATR): $\tilde{\nu}=3304$ (-NH-), 2972 ($-\text{CH}_2-$), 1643 cm^{-1} ($-\text{C}=\text{O}$); MS (MALDI-TOF): m/z (%) calcd for $\text{C}_{31}\text{H}_{40}\text{N}_2\text{O}_3\text{S}_4$: 616.92 $[M+H]^+$; found: 617.5.

S-TTF: A suspension of **S-2** (232 mg, 0.38 mmol) in freshly distilled triethyl phosphite (3 mL) under N_2 was heated to reflux for 2.5 h at 110°C. After cooling to room temperature, the reaction mixture was stirred overnight. Cold n -hexane was added to the reaction mixture and the orange precipitate was formed. The formed precipitate was collected by filtration and the crude precipitate was purified by column chromatography (silica gel, chloroform) and preparative HPLC to give pure **S-TTF**

as an orange powder (128 mg, 57%). FTIR (ATR): $\tilde{\nu}=3306$ (-NH-), 1533 (-NH-), 2930 ($-\text{CH}_2-$), 2955 ($-\text{CH}_2-$), 1495 ($-\text{C}_6\text{H}_5$), 1488 cm^{-1} ($-\text{C}_6\text{H}_5$); ^1H NMR (400.13 MHz, CDCl_3): $\delta=7.31$ (m, 20H, Ar-H), 6.10 (d, $J=8.00$ Hz, 4H, N-H), 5.09 (m, 4H, $-\text{COCNHCHCH}_3-$), 2.77 (t, $J=6.60$ Hz, 8H, $-\text{SCH}_2-$), 2.15 (t, 8H, $J=7.20$ Hz $-\text{CH}_2\text{CONH}-$), 1.62 (m, 18H, $-\text{SCH}_2\text{CH}_2-$, $-\text{CONHCHCH}_3-$), 1.46 ppm (m, 16H, $-\text{SCH}_2\text{CH}_2\text{CH}_2\text{CH}_2-$); ^{13}C NMR (100.61 MHz, CDCl_3): $\delta=21.85$, 25.22, 28.07, 29.19, 29.47, 36.51, 48.65, 126.20, 127.29, 127.75, 128.64, 143.44, 171.87 ppm; MS (MALDI-TOF): m/z (%) calcd for $\text{C}_{52}\text{H}_{90}\text{O}_4$: 1201.85 $[M+H]^+$; found: 1201.

R-1 was synthesized according to the same procedure as **S-1**.

Preparation of Helical Nanofibers

Helical nanofibers of **1** and F_4TCNQ were prepared by mixing a solution of **1** (0.23 mm) in hot toluene (1 mL) with a solution of F_4TCNQ (11.4 mm) in acetonitrile (20 mL). The loose gels were created after cooling. The color of the solution changed from orange to green by the formation of loose gels.

Electrical Conductivity

Temperature-dependent electrical conductivities of a cast film composed of **1** and F_4TCNQ were measured by using a DC two-probe method. Temperature-dependent DC conductivity and current-voltage (I - V) characteristics were measured using a homemade cryostat with a temperature control system over a range from 300 to 78 K. The current was monitored with a Keithley 6517 electrometer, with a constant bias voltage ranging from -100 to $+100$ V. Gold electrodes with 500 μm gap were formed by vacuum evaporation on glass substrate, followed by deposition of the films. Electrical contacts were constructed by using silver paste to attach with the 25 μm -diameter gold wires.

PCI-AFM Measurement

PCI-AFM measurements were carried out using a JSPM-5200 Environmental Scanning Microscope (JEOL, JSPM-4200) equipped with two function generators (NF, WF1946). Pt-coated conductive cantilevers with a force constant and resonant frequency of 7.5 Nm^{-1} and approximately 150 KHz, respectively, were used. Bias voltage (from -1.84 to $+1.84$ V) was applied to the gold electrode on the substrate with cantilever to be grounded. Both topographical and I - V data were obtained at 128×128 pixels. The measurements were carried out under nitrogen atmosphere at room temperature.

Acknowledgements

This work was supported by a project for "Creation of Innovation Center for Advanced Interdisciplinary Research Areas" in Special Coordination Funds for Promoting Science and Technology from the Ministry of Education, Culture, Sports, Science and Technology of Japan.

- a) J. W. Steed, J. L. Atwood, *Supramolecular Chemistry*, Wiley, Chichester, **2000**; *Perspectives in Supramolecular Chemistry* (Ed.: D. N. Reinhoudt), Wiley, Chichester, **1999**; b) J. Cornelissen, A. E. Rowan, R. J. M. Nolte, N. Sommerdijk, *Chem. Rev.* **2001**, *101*, 4039.
- a) S. I. Stupp, V. LeBonheur, K. Walker, L. S. Li, K. E. Huggins, M. Keser, A. Amstutz, *Science* **1997**, *276*, 384; b) T. Akutagawa, K. Kakiuchi, T. Hasegawa, S. I. Noro, T. Nakamura, H. Hasegawa, S. Mashiko, J. Becher, *Angew. Chem.* **2005**, *117*, 7449; *Angew. Chem. Int. Ed.* **2005**, *44*, 7283; c) C. Joachim, J. K. Gimzewski, A. Aviram, *Nature* **2000**, *408*, 541; d) J. C. Nelson, J. G. Saven, J. S. Moore, P. G. Wolyne, *Science* **1997**, *277*, 1793; e) P. Jonkheijm, P. van der Schoot, A. Schenning, E. W. Meijer, *Science* **2006**, *313*, 80.
- a) A. J. Epstein, S. Etemad, A. F. Garito, A. J. Heeger, *Phys. Rev. B* **1972**, *5*, 952; b) J. Ferraris, D. O. Cowan, V. Walatka, Jr., J. H. Perlstein, *J. Am. Chem. Soc.* **1973**, *95*, 948; c) R. L. Segura, N. Martin, *Angew. Chem.* **2001**, *113*, 1416; *Angew. Chem. Int. Ed.* **2001**, *40*, 1372.

- [4] P. Cassoux, D. de Caro, L. Valade, H. Casellas, S. Roques, J. P. Legros, *Synth. Met.* **2003**, *133–134*, 659.
- [5] a) A. R. Hirst, D. K. Smith, *Chem. Eur. J.* **2005**, *11*, 5496; b) M. Kimura, S. Kobayashi, T. Kuroda, K. Hanabusa, H. Shirai, *Adv. Mater.* **2004**, *16*, 335; c) J. Makarević, M. Jokić, Z. Raza, Z. Štefanić, B. Kojić-Prodić, M. Žinić, *Chem. Eur. J.* **2003**, *9*, 5567; d) K. Yoza, N. Amanokura, Y. Ono, T. Akao, H. Shinmori, M. Takeuchi, S. Shinkai, D. N. Reinhoudt, *Chem. Eur. J.* **1999**, *5*, 2722.
- [6] a) F. J. M. Hoeben, P. Jonkheijm, E. W. Meijer, A. P. H. J. Schenning, *Chem. Rev.* **2005**, *105*, 1491; b) A. R. Hirst, B. Escuder, J. F. Miravet, D. K. Smith, *Angew. Chem.* **2008**, *120*, 8122–8139; *Angew. Chem. Int. Ed. Engl.* **2008**, *47*, 8002–8018.
- [7] T. Kitahara, M. Shirakawa, S. Kawano, U. Bejín, N. Fujita, S. Shinkai, *J. Am. Chem. Soc.* **2005**, *127*, 14980.
- [8] T. Kitamura, S. Nakaso, N. Mizoshita, Y. Tochigi, T. Shimomura, M. Moriyama, T. Kato, *J. Am. Chem. Soc.* **2005**, *127*, 14769.
- [9] M. Hasegawa, H. Enozawa, Y. Kawabata, M. Iyoda, *J. Am. Chem. Soc.* **2007**, *129*, 3072.
- [10] a) C. Wang, D. Zhang, D. Zhu, *J. Am. Chem. Soc.* **2005**, *127*, 16372; b) Y. Tatewaki, Y. Noda, T. Akutagawa, R. Tunashima, S. Noro, T. Nakamura, H. Hasegawa, S. Mashiko, J. Becher, *J. Phys. Chem. C* **2007**, *111*, 18871; c) Y. Tatewaki, T. Akutagawa, T. Nakamura, H. Hasegawa, S. Mashiko, C. A. Christensen, J. Becher, *Colloids Surf. A* **2006**, *284–285*, 631; d) Y. Tatewaki, T. Akutagawa, T. Hasegawa, T. Nakamura, C. A. Christensen, J. Becher, *Mol. Cryst. Liq. Cryst.* **2004**, *424*, 17; e) Y. Tatewaki, T. Akutagawa, T. Hasegawa, T. Nakamura, J. Becher, *Synth. Met.* **2003**, *137*, 933.
- [11] a) N. Svenstrup, J. Becher, *Synthesis* **1995**, 215; b) K. B. Simonsen, J. Becher, *Synlett* **1997**, 1211; c) N. Svenstrup, K. M. Rasmussen, T. K. Hansen, J. Becher, *Synthesis* **1994**, 809.
- [12] a) T. Konuma, T. Akutagawa, T. Yumoto, T. Nakamura, J. Kawamata, K. Inoue, T. Nakamura, H. Tachibana, M. Matsumoto, K. Ikegami, S. Horiuchi, H. Yamochi, G. Saito, *Thin Solid Films* **1998**, *327–329*, 348; b) J. B. Torrance, B. A. Scot, B. Welber, F. B. Kaufman, P. E. Seiden, *Phys. Rev. B* **1979**, *19*, 730; c) S. Horiuchi, H. Yamochi, G. Saito, K. Sakaguchi, M. Kusunoki, *J. Am. Chem. Soc.* **1996**, *118*, 8604.
- [13] G. Saito, J. P. Ferraris, *Bull. Chem. Soc. Jpn.* **1980**, *53*, 2142.
- [14] a) M. Meneghetti, A. Girlando, C. Pecile, *J. Chem. Phys.* **1985**, *83*, 3134; b) A. Girlando, R. Bozio, C. Pecile, J. B. Torrance, *Phys. Rev. B* **1982**, *26*, 2306; c) H. Okamoto, Y. Tokura, T. Koda, *Phys. Rev. B* **1987**, *36*, 3858; d) M. Meneghetti, C. Pecile, *J. Chem. Phys.* **1986**, *84*, 4149.
- [15] a) A. Terahara, H. Nishiguchi, N. Hirota, H. Awaji, T. Kawase, S. Yoneda, T. Sugimoto, Z. Yoshida, *Bull. Chem. Soc. Jpn.* **1982**, *55*, 3896; b) J. B. Torrance, Y. Tomkiewicz, R. Bozio, C. Pecile, C. R. Eolf, K. Bechgaard, *Phys. Rev. B* **1982**, *26*, 2267; c) J. B. Torrance, J. J. Mayerle, K. Bechgaard, B. D. Silverman, Y. Tomkiewicz, *Phys. Rev. B* **1980**, *22*, 4960; d) J. B. Torrance, B. A. Scott, F. B. Kaufman, *Solid State Commun.* **1975**, *17*, 1369.
- [16] a) O. Hayashida, J. Ito, S. Matsumoto, I. Hamachi, *Chem. Lett.* **2004**, *33*, 994; b) T. Kobayashi, T. Seki, *Langmuir* **2003**, *19*, 9297.
- [17] a) J. H. Jung, Y. Ono, S. Shinkai, *Chem. Eur. J.* **2000**, *6*, 4552; b) J. H. Jung, Y. Ono, S. Shinkai, *Angew. Chem.* **2000**, *112*, 1931; *Angew. Chem. Int. Ed.* **2000**, *39*, 1862; c) J. H. Jung, H. Kobayashi, M. Mitsutoshi, T. Shimizu, S. Shinkai, *J. Am. Chem. Soc.* **2001**, *123*, 8785; d) S. K. Jha, K. Cheon, M. M. Green, J. V. Selinger, *J. Am. Chem. Soc.* **1999**, *121*, 1665; e) R. Cook, R. D. Johnson, C. G. Wade, D. J. O'Leary, B. Muñoz, M. M. Green, *Macromolecules* **1990**, *23*, 3454; f) M. M. Green, C. Khatri, N. C. Peterson, *J. Am. Chem. Soc.* **1993**, *115*, 4941.
- [18] a) H. Tanaka, Y. Okano, H. Kobayashi, W. Suzuki, A. Kobayashi, *Science* **2001**, *291*, 285; b) D. Jérôme, A. Mazaud, M. Ribault, K. Bechgaard, *J. Phys. Lett.* **1980**, *41*, 95; c) K. Bechgaard, K. Carneiro, M. Olsen, F. B. Rasmussen, C. S. Jacobsen, *Phys. Rev. Lett.* **1981**, *46*, 852.
- [19] a) S. Laschat, A. Baro, N. Steinke, F. Giesselmann, C. Hägele, G. Scalia, R. Judele, E. Kapatsina, S. Sauer, A. Schireivogel, M. Tosoni, *Angew. Chem.* **2007**, *119*, 4916; *Angew. Chem. Int. Ed.* **2007**, *46*, 4832; b) I. O. Shklyarevskiy, P. Jonkheijm, N. Stutzmann, D. Wasserberg, H. J. Wöndergem, P. C. M. Christianen, A. P. H. J. Schenning, D. M. de Leeuw, Z. E. Tomović, J. Wu, K. Müllen, J. C. Maan, *J. Am. Chem. Soc.* **2005**, *127*, 16233.
- [20] a) T. Akutagawa, T. Ohta, T. Hasegawa, T. Nakamura, C. A. Christensen, J. Becher, *Proc. Natl. Acad. Sci. USA* **2002**, *99*, 5028; b) T. Akutagawa, K. Kakiuchi, T. Hasegawa, T. Nakamura, C. A. Christensen, J. Becher, *Langmuir* **2004**, *20*, 4187.
- [21] a) A. Terawaki, Y. Otsuka, H. Y. Lee, T. Matsumoto, T. Kawai, *Appl. Phys. Lett.* **2005**, *86*, 113901; b) S. Yoshimoto, Y. Murata, K. Kubo, K. Tomita, K. Motoyoshi, T. Kimura, H. Okino, H. Hobara, I. Matsuda, S. I. Honda, M. Katayama, S. Hasegawa, *Nano. Lett.* **2007**, *7*, 956.
- [22] a) Y. Otsuka, Y. Naitoh, T. Matsumoto, T. Kawai, *Jpn. J. Appl. Phys.* **2002**, *41*, L742; b) H. Tanaka, T. Yajima, T. Matsumoto, Y. Otsuka, T. Ogawa, *Adv. Mater.* **2006**, *18*, 1411; c) Y. Otsuka, Y. Naitoh, T. Matsumoto, T. Kawai, *Appl. Phys. Lett.* **2003**, *82*, 1944.

Received: January 30, 2009
Published online: June 30, 2009